Electrochemical Characteristics of Carbon-coated Si/Cu/graphite Composite Anode

Hyung Sun Kim,* Kyung Yoon Chung, Won Il Cho, and Byung Won Cho

*Battery Research Center, Korea Institute of Science and Technology (KIST), P. O. Box, 131, Cheongryang, Seoul 130-650, Korea. *E-mail: kimhs@kist.re.kr*
Received February 5, 2009, Accepted May 22, 2009

The carbon-coated Si/Cu powder has been prepared by mechanical ball milling and hydrocarbon gas decomposition methods. The phase of Si/Cu powder was analyzed using X-ray diffraction (XRD), dispersive Raman spectroscopy, electron probe microanalysis (EPMA) and transmission electron microscope (TEM). The carbon-coated Si/Cu powders were used as anode active material for lithium-ion batteries. Their electrochemical properties were investigated by charge/discharge test using commercial $LiCoO_2$ cathode and lithium foil electrode, respectively. The surface phase of Si/Cu powders consisted of carbon phase like the carbon nanotubes (CNTs) with a spacing layer of 0.35 nm. The carbon-coated Si/Cu/graphite composite anode exhibited a higher capacity than commercial graphite anode. However, the cyclic efficiency and the capacity retention of the composite anode were lower compared with graphite anode as cycling proceeds. This effect may be attributed to some mass limitations in $LiCoO_2$ cathode materials during the cycling.

Key Words: Si/Cu/graphite composite anode, Carbon nanotube, Lithium ion battery

Introduction

Recently, many anode materials have been studied in order to meet the requirement of high specific capacity for lithium ion batteries. Among the candidate anode active materials, silicon is one of the most attractive materials due to its high theoretical specific capacity in comparison with the conventional graphite materials.[1,2] However, most Li/Si alloys are usually pulverized by the large volume change during the electrochemical lithiation/delithiation process, which results in the loose electrical connection between the active materials and current collector substrate. This effect became the main reason of capacity fading preventing from applying to commercial lithium-ion battery. Many attempts have been made to overcome these problems by the surface modification of the silicon powders with different techniques.[3-5] It has been also reported that the alloying of silicon with copper metal limits alloying of lithium with silicon or buffers the volume change of the silicon during electrochemical cycling.[6,7] In this work, in order to improve the cycling performance of Si-based anode, we have synthesized a new carbon-coated Si/Cu/graphite composite anode by mechanical ball milling and hydrocarbon gas decomposition methods. Its effect on the electrochemical properties was investigated using various analytical methods.

Experimental

Microsized Si and Cu powders (under 325 mesh, Aldrich) were mixed with a weight percent of 95:5 and then put into zirconia bowl. The bowl was evacuated and filled with pure argon gas in a glove box. The ball milling process was performed in a planetary machine (Pulverisette 7, Fritsch) at a rotation speed of 400 rpm for 5 h and then, followed in wet ball milling for 5 h with ethyl alcohol solvent to reduce powder size. The carbon phase was formed on the surface of Si/Cu powders. It was prepared by pyrolysis of the powder mixture in an alumina boat at 700 °C for 10 h under gas flow of argon containing 10 mol% propylene gas. The obtained powders were identified and examined by XRD (Rint/Dmax-2500, Rigaku), dispersive Raman spectroscopy (Nicolet Almega XR, Thermo Electron Corp.), TEM (Tecnai 2, FEI Hong Kong Co., Ltd.) and EPMA (JXA8500F, JEOL). The carbon-coated Si/Cu/graphite composite powders were prepared by mixing spherical natural graphite powder (size: 18 μm, Sodiff Co., Ltd.) and the carbon-coated Si/Cu powder with a weight ratio of 9 : 1. The composite anode used carbon-coated Si/Cu/graphite as the active material, Denka carbon black (Denki Kagaku K. K., Japan) as the conductive agent, and styrene butadiene rubber (40 wt% in water, Zeon) and sodium carboxymethyl cellulose (1 wt% in water, Sigma) mixture as the binder. Measured amounts of the above materials were introduced in stainless steel cup according to the electrode formulation of 92.1 wt% active material, 4.6 wt% carbon black, and 3.3 wt% binder. A homogenizer was used to rotate the cup at 3000 rpm for 30 min. Then, the slurries were cast on a copper foil and dried at 80 °C in oven for several hours to remove water solvent. The composite anode and commercial graphite anode (dimension: 3 × 4 cm) were punched from the coated copper foil and dried at 80 °C in vacuum oven for 24 h, respectively. They were assembled in aluminum plastic pouches with lithium foil electrode or commercial $LiCoO_2$ cathode as counter electrode at dry room (dew point: -60 °C), respectively. A microporous polypropylene separator (Celgard 2400) was used. The electrolyte used was 1 M $LiPF_6$ in mixed solvent of ethylene carbonate, ethyl-methyl carbonate, dimethyl carbonate (volume ratio 1:1:1), and 2 vol% vinylene carbonate as an electrolyte additive. Electrochemical cycling was performed galvanostatically between 0.005 V and 1.0 V *vs.* Li/Li^+ for the half cell, and between 3 V and 4.2 V *vs.* Li/Li^+ for the full cell using Maccor battery test system (Series 4000, USA), respectively.

Results and Discussion

Fig. 1 shows the XRD pattern of the pyrolyzed Si/Cu powder. Si/Cu composite powder consists of crystalline silicon and $Cu_{15}Si_4$ alloy. We guess from the results of XRD analysis that copper embeds into the crystalline silicon lattice to form the $Cu_{15}Si_4$ alloy phase during the pyrolysis under argon mood. Fig. 2 shows the Raman spectrum of the pyrolyzed Si/Cu powder. This spectrum was recorded with a 633.0 nm excitation line. The sharp peaks centered at approximately 520 cm^{-1} and 930 cm^{-1} correspond to the typical crystalline silicon phases, while the two broad peaks at 1350 cm^{-1} and 1590 cm^{-1} are related to the carbon phase. In the spectrum of a pure carbon film, the position of D (disordered carbon) and G (graphitic carbon) bands was 1340 cm^{-1} and 1582 cm^{-1}. The positions and relative intensities of the G and D bands provide more information on the structure and domain size of a carbon material.[8] The two peaks indicate that the carbon layer is composed of crystalline graphitic and amorphous carbon phase. TEM analysis was performed on the pyrolyzed Si/Cu powder to identify carbon layer structure and was shown in Fig. 3. The outer surface of Si/Cu powder is covered with carbon phase like CNTs patterns and the average spacing layer of the grown CNTs is about 0.35 nm. The hydrocarbon gas first decomposes on the surface of the copper catalytic particle, and then the carbon precipitates out on the surface of the silicon particle to form CNTs. Fig. 4 presents EPMA image of the pyrolyzed Si/Cu powder. The size of the agglomerates is less than submicron. Silicon particles and carbon materials are much smaller compared with copper particles. These powders are distributed randomly due to the low content of copper particles. However, copper particles adhere tightly to the surface of silicon particles enclosed by the pyrolyzed carbon. This encapsulation may give a good electrical contact between active particles and current collector and also provide a buffering effect for volume change during cycling.[9] Fig. 5 shows the voltage profiles of the carbon-coated Si/Cu/graphite composite anode and pure graphite anode using commercial $LiCoO_2$ cathode at the 10th cycle, respectively. In case of the pure graphite anode, the charge capacity and the discharge capacity are 33 mAh and 31 mAh.

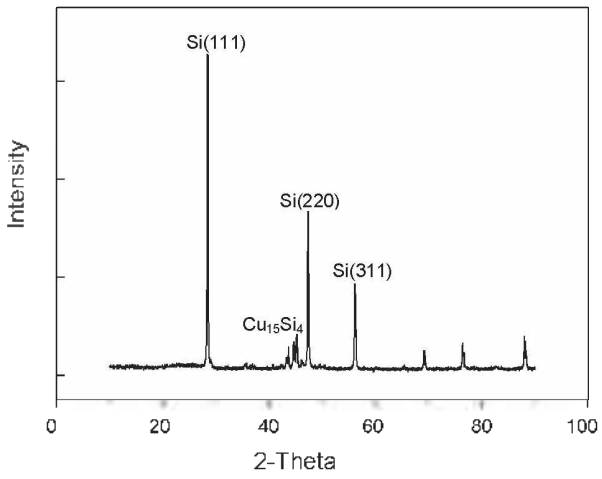

Figure 1. XRD pattern of pyrolyzed Si/Cu powder.

For the carbon-coated Si/Cu/graphite composite anode, although the average working potential is lower compared with pure graphite anode due to the silicon anode, the charge capa-

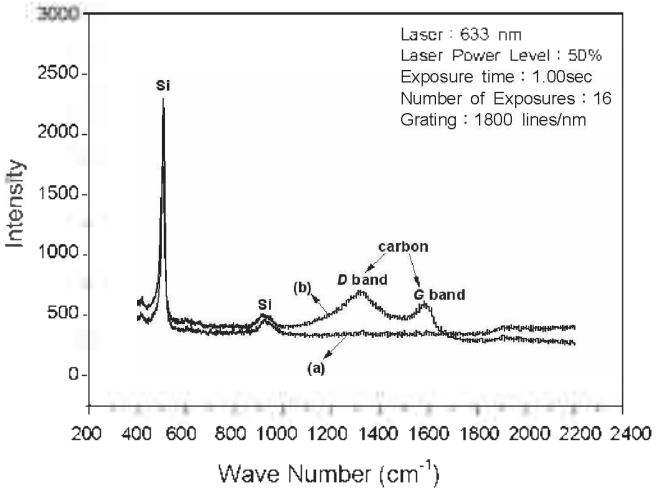

Figure 2. Raman spectrum of Si/Cu powder (a) and pyrolyzed Si/Cu powder (b).

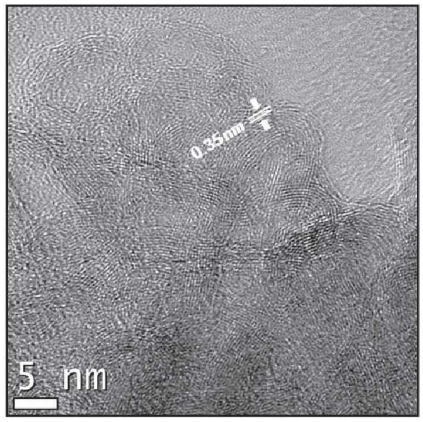

Figure 3. TEM image of pyrolyzed Si/Cu powder.

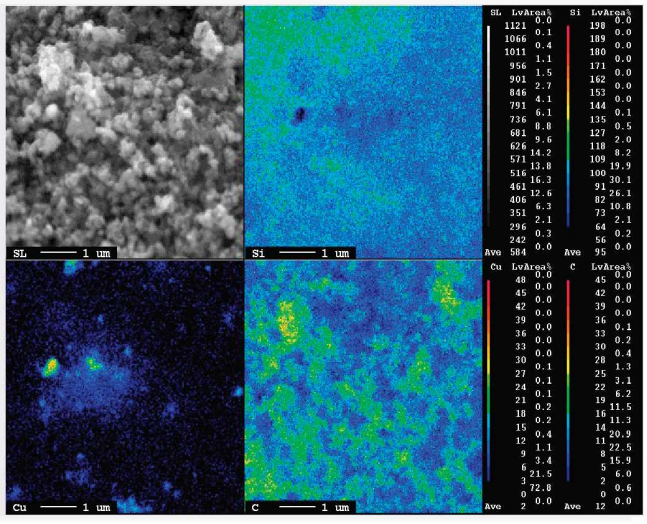

Figure 4. EPMA image of pyrolyzed Si/Cu powder.

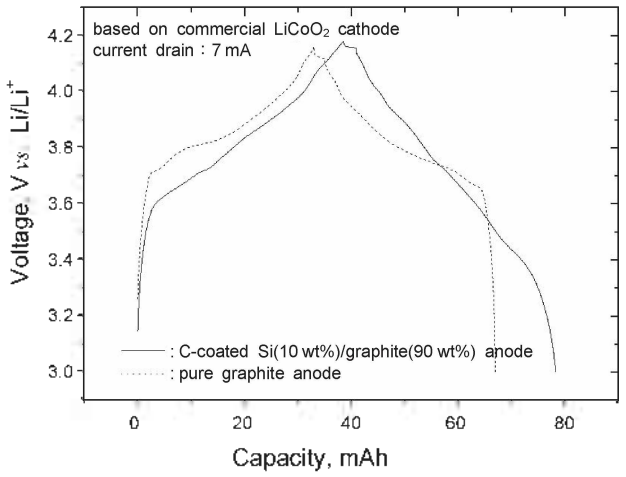

Figure 5. Voltage profiles of carbon-coated Si/Cu/graphite and graphite anode using $LiCoO_2$ cathode at 7 mA current rate.

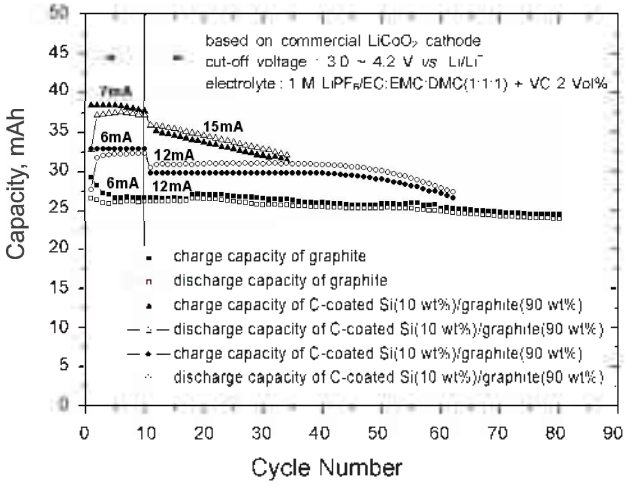

Figure 6. Cycling performances of carbon-coated Si/Cu/graphite and graphite anode using $LiCoO_2$ cathode at various current rates.

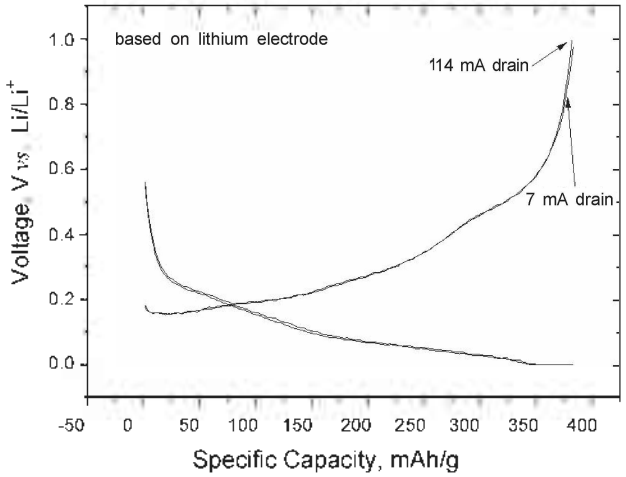

Figure 7. Voltage profiles of carbon-coated Si/Cu/graphite composite anode using lithium electrode at different current rates.

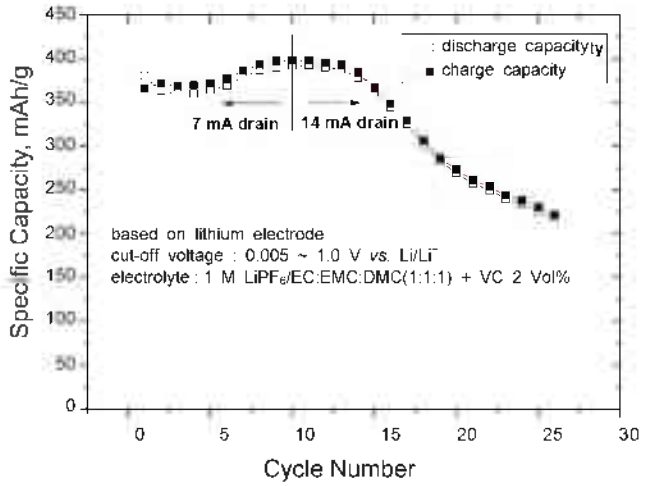

Figure 8. Cycling performances of carbon-coated Si/Cu/graphite composite anode using Li electrode at different current rates.

city and the discharge capacity increased to 38 mAh and 36 mAh. It was reported that the average working voltage of the carbon-coated Si/$LiCoO_2$ cell was *ca* 3.4 V *vs.* Li/Li$^+$.[10] This value is *ca* 0.3 V lower than the working voltage of the corresponding cells using graphite anode materials. As demonstrated above, the total capacity of 38 mAh and 36 mAh corresponds to the specific capacity of 413 mAh/g and 390 mAh/g based on the weight of Si/Cu/graphite active materials, respectively. Fig. 6 shows the cycling performances of the carbon-coated Si/Cu/graphite composite anode and pure graphite anode using commercial $LiCoO_2$ cathode at different current rates. The cells were charged to 4.2 V and discharged to 3 V *vs.* Li/Li$^+$ by constant currents. The total capacity of carbon-coated Si/Cu/graphite composite anode is higher than that of pure graphite anode, especially at high current rate (7mA). In theses cells, however, the high coulombic efficiency and capacity retention as commercial graphite anode could not be obtained during the cycling. This may be due to the irreversible capacity loss of Si anode materials or some mass limitation in $LiCoO_2$ cathode materials. In order to further understand the reason, we performed half cell test using lithium foil electrode instead of $LiCoO_2$ cathode at different current rates. The cell was discharged to 0.005 V and charged to 1.0 V *vs.* Li/Li$^+$. A good coulombic efficiency and stable charge/discharge characteristics could be obtained irrespective of current rates as shown in Fig. 7. However, the specific capacity of carbon-coated Si/Cu/graphite composite anode decreased suddenly due to the formation of unstable solid electrolyte interphase on the surface of lithium electrode after 15 cycles as shown in Fig. 8. As a result, it could be deduced that the main reason of the capacity fading and low cyclic efficiency in the carbon-coated Si/Cu/graphite anode was attributed to the mass limitation of $LiCoO_2$ cathode. Although the carbon-coated Si/Cu/graphite composite anode was discharged to 0.005 V *vs.* Li/Li$^+$, it wasn't detected plateau potential at about 0.45 V *vs.* Li/Li$^+$ in the charge process as our previous study.[11] In this case, copper metal limits alloying of lithium with silicon. Therefore, cycling silicon anode even below 0.05 V *vs.* Li/Li$^+$ avoids the formation of crystallized phase and results in good cycling performance. This crystallized phase was identified as $Li_{15}Si_4$.[12] Delithiation of the $Li_{15}Si_4$ phase results in the formation of amorphous silicon.

Conclusion

A carbon-coated Si/Cu composite powder was synthesized by mechanical ball milling and hydrocarbon gas decomposition at high temperature. After that, the surface phase of Si/Cu power was covered with carbon layer like typical CNTs patterns. Silicon powder, copper particle and carbon material were distributed randomly within the pyrolyzed composite powder. The carbon-coated Si/Cu/graphite composite anode exhibited a higher capacity than that of commercial graphite anode. However, the cyclic efficiency and the capacity retention of the composite anode were lower compared with conventional graphite anode due to the mass limitation of $LiCoO_2$ cathode. Even though the carbon-coated Si/Cu/graphite composite anode was discharged to 0.005 V *vs.* Li/Li^-, it wasn't detected the plateau potential at about 0.45 V *vs.* Li/Li^+ during the charging.

Acknowledgments. This work was supported financially by "Development of Basic Technologies for Large-Scale Lithium Secondary Batteries for Plug-in Hybrid Electric Vehicle" project of KIST.

References

1. Netz, A.; Huggins, R. A.; Weppner, W. *J. Power Sources* **2003**, *119-121*, 95.
2. Kim, I.; Blomgren, G. E.; Kumta, P. N. *Electrochemical and Solid-State Letters* **2003**, *6*, A157.
3. Kim, H.; Chung, K.; Cho, B. *J. Power Sources* **2009**, *189*, 108.
4. Dimov, N.; Kugino, S.; Yoshio, M. *Electrochimica Acta* **2003**, *48*, 1579.
5. Shi, D. Q.; Tu, J. P.; Yuan, Y. F.; Wu, H. M.; Li, Y.; Zhao, X. B. *Electrochemistry Communications* **2006**, *8*, 1610.
6. Zuo, P.; Yin, G.; Hao, X.; Yang, Z.; Ma, Y.; Gao, Z. *Materials Chemistry and Physics* **2007**, *104*, 444.
7. Kim, J.; Kim, H.; Sohn, H. *Electrochemistry Communications* **2005**, *7*, 557.
8. Zhang, Z.; Dewan, C.; Kothari, S.; Mitra, S.; Teeters, D. *Materials Science and Engineering B* **2005**, *116*, 363.
9. Liu, Y.; Hanai, K.; Yang, J.; Imanishi, N.; Hirano, A.; Ichikawa, T.; Takeda, T. *Electrochemical and Solid-State Letters* **2004**, *7*, A369.
10. Yoshio, M.; Wang, H.; Fukuda, K.; Umeno, T.; Dimov, N.; Ogumi, Z. *J. Electrochem. Soc.* **2002**, *149*, A1598.
11. Kim, H.; Chung, K.; Cho, B. *Bull. Korean Chem. Soc.* **2008**, *29*, 1965.
12. Obrovac, M.; Christensen, L. *Electrochemical and Solid-State Letters* **2004**, *7*, A93.